RSC Advances

This article can be cited before page numbers have been issued, to do this please use: Y. Luo, J. Ran, R. Chen and X. cheng, *RSC Adv.*, 2016, DOI: 10.1039/C6RA17790E.

ROYAL SOCIETY OF CHEMISTRY

www.rsc.org/advances

View Article Online
DOI: 10.1039/C6RA17790E

Facile Synthesis of Porous Organic Polymers for the Absorption of Pd(Ⅱ) Ions and Organic Dyes

Yanmei Luo[a], Junhui Ran[a], Rong Chen[b], and Xinjian Cheng[a*]

[a]School of Textiles and Garments, Southwest University, Chongqing, P. R. China, 400715

[b]School of Chemical Engineering and Pharmacy, Wuhan Institute ofTechnology, Wuhan, P. R. China 430073

Abstract: Porous organic polymers (POPs) were prepared via two-step reactions. In the first step, dialdehyde compounds were synthesized by Suzuki-Miyaura coupling reaction. And in the second step, the dialdehyde compounds reacted with hydrazine hydrate to form polymers by the Schiff's base formation reactions. These POPs are layer-nanosheet structured, crystalline and fluorescent. They are studied by FTIR, Fluorescence spectra, UV-Vis, SEM, TEM, XRD, DSC, and TGA. It is found that the pore parameters, such as specific surface areas and pore diameters of the POPs could be adjusted by changing the reaction time and temperature. The specific surface areas increased with the increasing of reaction time and temperature. The maximum specific surface area could reach 715.6 m^2/g. Furthermore, the POPs could detect and remove Pd(Ⅱ) ions and organic dyes. When contact with Pd(Ⅱ) ions, the fluorescence of the POPs quenched, and the POPs could absorb Pd(Ⅱ) ions as well. The maximum absorption capacity for Pd(Ⅱ) ions could reach 20.6 mg/g within 5min.

* Corresponding author, Dr. Cheng, chxj606@163.com

View Article Online
DOI: 10.1039/C6RA17790E

Meanwhile, the POPs could absorb two model dyes, rhodamine B (RhB) and methylene blue (MB), with high efficiency within 5min.

Keywords: POPs nanosheet, absorption of Palladium ions, absorption of organic dyes

View Article Online
DOI: 10.1039/C6RA17790E

1. Introduction

In recent years, organic dyes and heavy metal ions are becoming serious pollutants to environments and creatures with the development of the industry. Palladium is often employed as high-performance catalyst in most organic reactions. And sometimes the pollutions caused by Pd are neglected. Pd could lead to disease when it is enriched in human body. Rhinoconjunctivitis, allergy and asthma could be caused by it[1]. Therefore, detection and recycling of Pd ions are very important.

Fluorescent sensors have attracted considerable attention due to their ability to detect and remove some metal ions. Some chemosensors have been proved can detect Pd(Ⅱ)ions with high sensitivity and selectivity[2-4].Ezoddin et al [5] have prepared hydrophilicity-switchable solvent for the recognition of palladium by air-assisted liquid-liquid micro-extraction. The recognition limit value reaches 0.07 μg/L. Yan et al [6] have synthesized a fluorometric and colorimetric NBD-PMA chemosensor for selective detection of palladium(Ⅱ) ions. These sensor could selectively coordinate with palladium(Ⅱ) ions with a color change from yellow to pink. And the change could be detected by the naked eyes. In our previous work, fluorescent nanoparticles and glass were prepared and used for detection and removal of Pd(Ⅱ) ions[7]. In addition, fluorescent conjugated polymers have attracted much attention due to the "molecular wire" effect. When contact with metal ions, the fluorescence could be magnified. These conjugated polymers could detected Pd ions with high sensitivity. Bai's group [8, 9] have prepared this kind of conjugated polymers for the detection of palladium ions.

View Article Online
DOI: 10.1039/C6RA17790E

Organic dyes are widespread because of their splendid colors with the development of garments industry. Meanwhile, they are hazardous materials to our water resource, soils and atmosphere.For the treatment of organic dye pollutants, degradation and adsorption are the frequently used methods. For example, in our previous work[10], a composite nano-fiber mat was prepared and employed to treat MB pollutants. The mat could photo-degradeMB under UV light. Zhu et al.[11] have prepared porous coordination polymers for the degradation of organic dyes. The as-prepared porous polymers could treat rhodamine B (RhB), methylene blue (MB) and safranine T (ST), the dyes degraded in neutral aqueous solution with high efficiency.

Porous organic polymers (POPs) have attracted much attention due to their unique structures. Most POPs have large surface area[12], high chemical stabilities and low skeleton density[13].They can be applied to gas storage and separation [12-15], adsorption of CO_2[15-18], catalysis[19-22] and chemical sensing[23-25]. For example, Yu et al[13] have synthesized microporous polyphenylenes via ethynyl trimerization reaction with aromatic ethynyl monomers. Their pore diameter and BET surface areas reached 0.7 nm and 1246 m^2/g respectively.These microporous polyphenylenes could be used to store hydrogen. In general, POPs have porous network structures or three-dimensional organic frameworks.This structure provides a wide interface for gas capture, so POPs can be used as chemosensor[26-30]for many chemicals. Conjugated microporous polymers were prepared by Adams et al[28] via Ni-catalyzed Yamamoto polymerization between 1,3,6,8-tetrabromopyrene and 1,4-dibromobenzene. The as-prepared microporous polymers have high luminescence and the emission colour

View Article Online
DOI: 10.1039/C6RA17790E

could be tuned by introducing varying comonomers. Most of POPs have π-conjugated characteristics so that they are sensitiveto electron-deficient compounds[31-34]. Zheng et al [35] have synthesized POPs with high thermostability due to the rigid macro-cyclic structures. Suh et al [36] have synthesized POPs of considerable surface areas (830 m^2/g) with as high CO_2 capture ability as 3.14 mmol/g.In addtion, chang et al [37] have synthesized indole-based microporous organic polymer by the reaction of 1,3,5-tris-(4-fluorobenzoyl)benzene and 3,3′-diindolylmethane via nucleophilic substitution reaction. The preparative strategy of the microporous organic polymer exhibits cost-effective advantages. The polymer have considerable BET surface area (2090 m^2/g), large adsorption capacity (16.0 wt%) for carbon dioxide and hydrogen storage (2.48 wt%). Its good performance shows application vision in the environmental technology. Moreover, mannitol-based and ketal-linked porous organic polymers were prepared by Ding et al [38]through condensation reaction between mannitol and aromatic acetyl monomers. They demonstrated high carbon dioxide uptake (11.5 wt%) due to hydroxyl-rich structures and the predominant micropores.

In this work, two fluorescent POPs were prepared.They exhibited sensing and separation ability to Pd ions. Also they exhibited high-performance to absorb organic dyes. Firstly, two intermediate dialdehydes were prepared with 1,4-benzenediboronic acid and 4-bromobenzaldehyde by Suzuki-Miyaura coupling reaction. And then, two porous organic polymers was synthesized via Schiff's base formation reaction. In the process of polymerization, POPs (two kinds of polymers are named as P**1** and P**2** series) were obtained. P**1** and P**2** exhibit excellent ability to detect Pd(Ⅱ) ions, the

View Article Online
DOI: 10.1039/C6RA17790E

fluorescence quenched dramatically when contact Pd(Ⅱ) ions. In addition,these POPs could rapidly absorb organic dyes in aqueous solution with high efficiency.

2. Experimental section

2.1 Materials

6-bromo-3-pyridinecarboxaldehyde, 4-bromobenzaldehyde, 1,4-benzenediboronic acid, tetrakis(triphenylphosphine)palladium(0),hydrazine hydrate, rhodamine B, and methylene blue were purchased from J&K China Chemical Ltd. All metal salts (Fe(Ⅲ), Cr(Ⅲ), Mn(Ⅱ), Co(Ⅱ), Cd(Ⅱ), Zn(Ⅱ), Ag(Ⅰ), Pb(Ⅱ), Ca(Ⅱ), Ni(Ⅱ), Cu(Ⅱ), Na(Ⅰ), K(Ⅰ), Hg(Ⅱ), Mg(Ⅱ), Fe(Ⅱ) and Pd(Ⅱ)) were purchased from Aladdin chemical co., Ltd and used as received. All solvents were also purchased from Aladdin chemical co., Ltd. They were dried before using.

2.2 Synthesis of 4''-Aldehyde-[1,1',4',1'']terphenyl-4-carbaldehyde (compound 1) and 6-[4-(5-Aldehyde-pyridin-2-yl)-phenyl]-pyridine-3-carbaldehyde (compound 2)

Compound **1** was prepared by Suzuki-Miyaura coupling reaction[39] using the following procedure: mix 4-bromobenzaldehyde (1 mmol), 1,4-benzenediboronic acid (0.6 mmol), Na_2CO_3 (1.5 mmol) in deionized water (10 mL) and DMF (10 mL) with nitrogen atmosphere at room temperature. After being stirred for 0.5 h, tetrakis(triphenylphosphine)palladium(0) (0.1% mmol) was added. The reaction mixture was stirred for 8h at 80 ℃. Thereafter, the mixture was extracted with trichloromethane (20 mL, 3 times). The extract was dried by the anhydrous Na_2SO_4, and then the solvent was evaporated to obtain crude product. It was purified through

View Article Online
DOI: 10.1039/C6RA17790E

column chromatography with $CHCl_3$/petroleum ether as eluent. White solid was obtained, its yield was 72.5%. ^{1}H NMR spectra data (Supporting information, Fig. S1) of compound **1** are as follows (DMSO-d_6, 600 MHz): 10.079 (s, 2H), 8.027 (s, 8H), 7.945 (s, 4H). Using the same procedure, Compound **2**was obtained, its yield was 53.2%. ^{1}H NMR spectra data (Fig. S2) of compound **2** are as follows (DMSO-d_6, 600 MHz): 10.168 (s, 2H), 9.207(d, 2H), 8.394 (s, 6H), 8.336 (s, 2H).

2.3 Synthesis of porous organic polymericnano-sheet

POP nanosheet (P**1**) was synthesized with the reaction between compound **1** and hydrazine hydrate (0.98 : 1, molar ratio) in DMF. Four different reaction conditions were investigated and different products were obtained. That is under 80^{o}C for 24h (named as P**1**-1), under 160^{o}C for 24h (named as P**1**-2), under 160^{o}C for 40h (named as P**1**-3), and under 160^{o}C for 24h (named as P**1**-4) respectively. The crude product were washed by DMF and water for three times. The other series of porous organic polymer nano-sheet (P**2-1** to **P2-4**) was synthesized using the same method.

2.4 Characterization

^{1}H NMR was analyzed by AVANCE III 600 MHz instrument (Bruker), Fourier transform infrared spectra (FTIR, 4000-400cm^{-1}) were performed on a Nicolet NEXUS 470 spectrometer. Fluorescence spectra were measured on a Shimadzu F-4600 FL spectrophotometer. UV-Vis absorption was measured on a UV-5900PC spectrophotometer (METASH). Differential scanning calorimetry was measured by DSC 214 Polyma instrument. The POPs were observed by the scanning electron microscopy (SEM, JEOL JSM-7600F) and Transmission electron microscope (TEM,

View Article Online
DOI: 10.1039/C6RA17790E

JEOL JEM-2100). Zeta potentials were recorded on a Zeta Plus S/N21479 (Brookhaven Instrument Corporation). Thermogravimetric Analysis (TGA) was conducted on a 209F3 Tarsus NETZSCH instrument. Porous structure was analyzed by BET (Quantachrome Instruments version 4.01). Elemental analysis were measured by a Elementar Vario Micro Select instrument (Germany). Atomic Absorption spectrometry (AAS) were measured by an ICP single channel scanning spectrometer (Z-5000).

3. Result and discussion

3.1 Synthesis and characterization of P1 and P2

The synthesis procedure of POPnanosheet (P**1** and P**2**) was presented in **Scheme 1**. In step 1, compound **1** was prepared via Suzuki-Miyaura coupling reaction between 4-bromobenzaldehyde and 1,4-benzenediboronic acid. Compound 2 was also prepared via Suzuki-Miyaura reaction between 1,4-benzenediboronic acid and 6-bromo-3-pyridinecarboxaldehyde. Instep 2, POPs(P**1** and P**2**) were prepared via polycondensations between compound **1**/compound **2** and hydrazine hydrate.

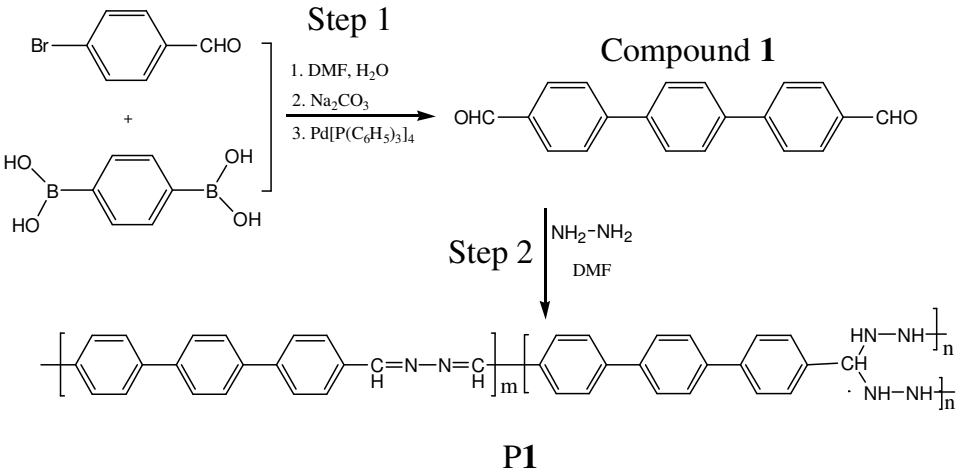

Scheme. 1 Synthesis procedure of compound **1** and P**1**.

View Article Online
DOI: 10.1039/C6RA17790E

P**1** and P**2** couldn't be dissolved incommon solvents, such as DMF, DMSO, ethanol, methanol, THF, acetone, trichloromethane and dichlormethane and so on. The structures of compound **1,**compound **2,**P**1,** and P**2** were confirmed by FTIR and shown in Fig. 1. The strong absorption bands of aldehyde groups in compound **1** and compound **2** at 1687 cm^{-1}could be seen clearly. When the polymers were formed, peaks at 1687 cm^{-1} became weaker, it indicated aldehyde groups reacted with NH_2NH_2. Besides, the characteristic absorption of imine linkage (-C=N-), aliphatic (-C-N-) and amine (N-H) were observed at 1620 cm^{-1}, 1217 cm^{-1} and 3380 cm^{-1}.These peaks further confirmed the successful preparation of the POPs.

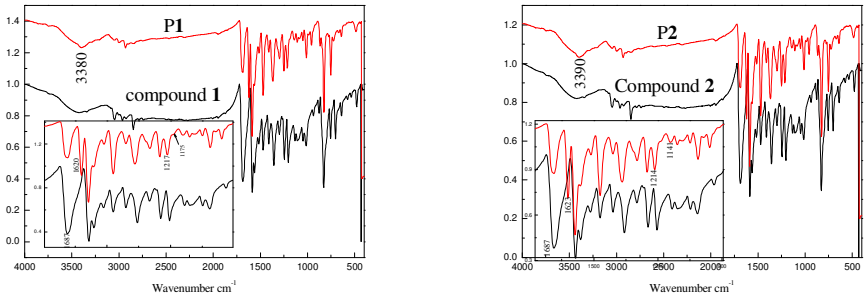

(a) (b)

Fig. 1 FTIR spectra of (a) compound **1**and P**1** and (b) compound **2** and P**2**.

The elemental analysis data of P**1** and P**2** were listed in the table **1**. It can be seen that the measured mass fractions (in P**1)** of C, H and N elemental were 84.0%, 5.2% and 10.6% respectively. Similarly, in table **1**, the elemental composition data of P**2** was displayed. It indicated the measured mass fractions (in P**2**) of C, H and N elemental were 72.2%, 4.5% and 16.8% respectively. However, according to the theoretical calculation,ifthere was only C=N bond in the P**1**, the mass fraction of C, H and N elemental should be 85.1%, 5.0% and 9.9%. While ifthere was only C-N in the

View Article Online
DOI: 10.1039/C6RA17790E

P**1**, the mass fraction of C, H and N elemental should be 76.5%, 5.7% and 17.8% respectively. These data indicated that there were both -C-N-bond and -C=N- bond in P1. Similarly, there were both C-N bond and C=N bond in P2.

Table 1 The elemental analysis of P**1** and P**2**.

Entry	C(%)	H(%)	N(%)
P**1**	84.0	5.2	10.6
P**2**	72.2	4.5	16.8

3.2 The morphology, structure and thermostability of P1 and P2

To study the morphology and structure of materials, SEM and TEM are often employed [40, 41]. SEM and TEM photographs of P**1** and P**2** were obtained and shown in **Fig. 2**. From the high resolution TEM, the sheets of POPs could be seen clearly. And by the selected area electron diffraction (SAED) pattern (inset in Fig. 2a), the crystalline structures could be observed. However, compared with some inorganic mareriaals, the difraction pattern is weaker. For the sake of more accuracy, X-ray diffraction measurement was conducted in the following. From Fig. 2b, c, d, e and f, it could be seen that P**1** and P**2** exhibit layered nanosheet structures, and the layers are parallelly pilled up. There were many pores between the layers. The distance between layersof P**1**-2, P**1**-3, **P2**-1, P**2**-2 and P**2**-3 were approximately calculated. And they are 44±5nm, 32±5nm, 68±5nm, 42±5nm and 30±5nm respectively. The results indicated that the distance between layers decreased with the increase of reaction time and reaction temperature.

View Article Online
DOI: 10.1039/C6RA17790E

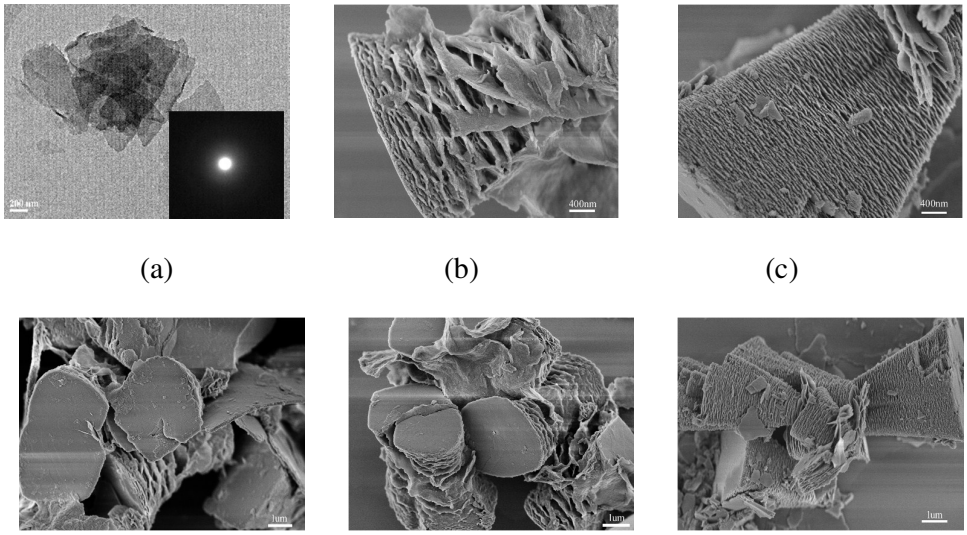

(a) (b) (c)

(d) (e) (f)

Fig. 2TEM (inset is the diffraction Pattern) image of (a) P**1**-1, and SEM of (b) P**1**-2, (c) P**1**-3, (d) P**2**-1, (e) P**2**-2 and (f) P**2**-3.

XRD measurements of P**1** and P**2** were conducted.And the data were measured at a scanning rate of 4° min^{-1} in the 2θ range of 5° to 70°. In Fig. 3, P1 and P2 show sharp peaks, it indicates the crystalline structures. P1 and P2 possess three peak at 2θ values of about 20°/20°, 23°/25° and 28°/30°.

View Article Online
DOI: 10.1039/C6RA17790E

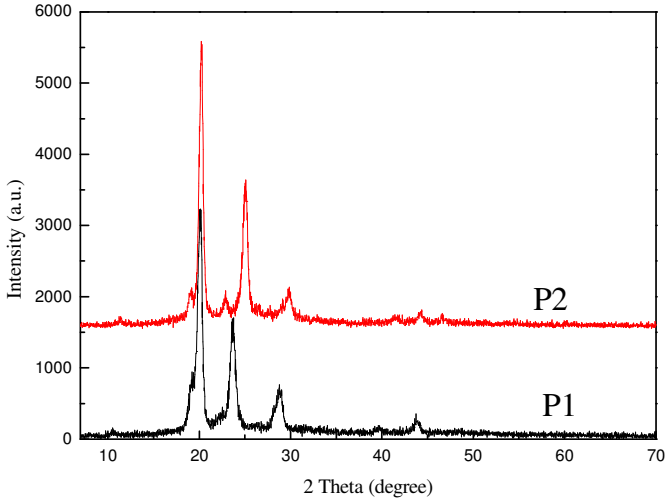

Fig. 3 Powder X-ray diffraction of P**1** and P**2**.

Compound **1**, compound **2,** P**1**, and P**2** were investigated by TGA under N_2 atmosphere. As shown in the **Fig. 4 (a)**, the decomposing temperature of compound **1** was 311 ^{o}C, the decomposing temperature of the polymers were 408 ^{o}C. It indicated the high thermal stability of P**1** when compound **1**waspolymerized. Similarly, thermal stability of P**2** (402 ^{o}C) were higher than compound **2** (300 ^{o}C).

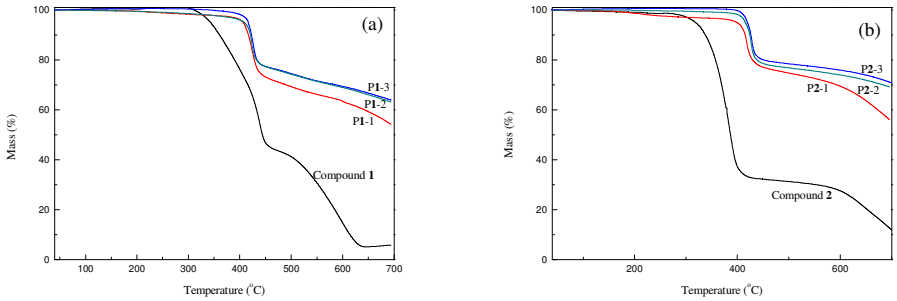

Fig. 4 TGA cures of (a) compound **1**, P**1**-1, P**1**-2 and P**1**-3 and (b) compound **2**, P**2**-1, P**2**-2 and P**2**-3.

Differential scanning calorimetry (DSC) curves of P**1** and P**2** were analyzed at a heating rate of 10 °C min^{-1} in the temperature range of -50 ^{o}C to 500^{o}C. Each sample

View Article Online
DOI: 10.1039/C6RA17790E

was tested for three times. As shown in the **Fig. 5**, there is not a noticeable glass transition for P**1**. This may be caused by a relatively high degree of cross-linking. There was a exothermic peak at 418 ^{o}C, it could be attributed to the crystallization. In addition, there was a glass transition peak for P**2** at 85 ^{o}C and at a crystallization peak at 410 ^{o}C.

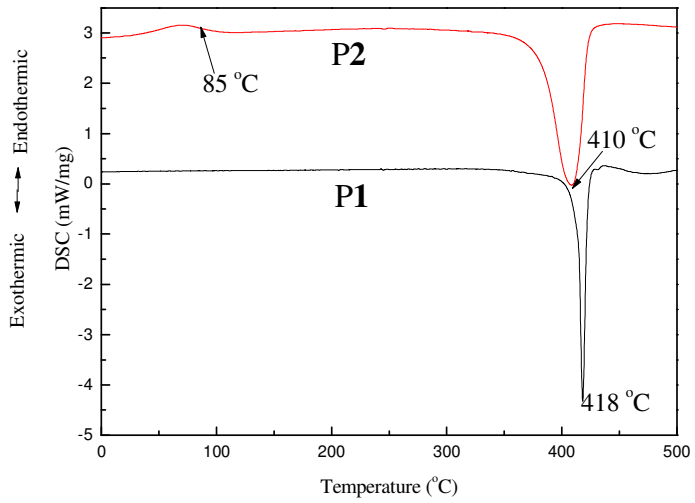

Fig. 5 Differential Scanning Calorimetry (DSC) analysis of P**1** and P**2**.

The zeta potentials of P**1** and P**2** were measured in the range of pH from 2 to12. When P**1** and P**2** were in a lower pH value, the protonation on the N atoms occurred, and the nano-sheets were positively charged. And in a higher pH value, the deprotonation on the N atoms occurred, the nano-sheets were negatively charged. As shown in the **Fig. S3**, zeta potential *vs*pH curves were plotted. P**1** and P**2** have almost the same isoelectric points of 4.4 and 4.3.

3.3 Porous Structure of Polymers (P1 and P2)

View Article Online
DOI: 10.1039/C6RA17790E

The porous structures of polymers (P**1** and P**2**) were measured by nitrogen sorption at 77 K (**Fig. 6**), which revealed P**1** and P**2** are of the mesoporous structures. And indicated typical type-Ⅲ mesoporous materials. The isotherms of all POPs exhibited the adsorbing volumes increased with the increase of relative pressure.

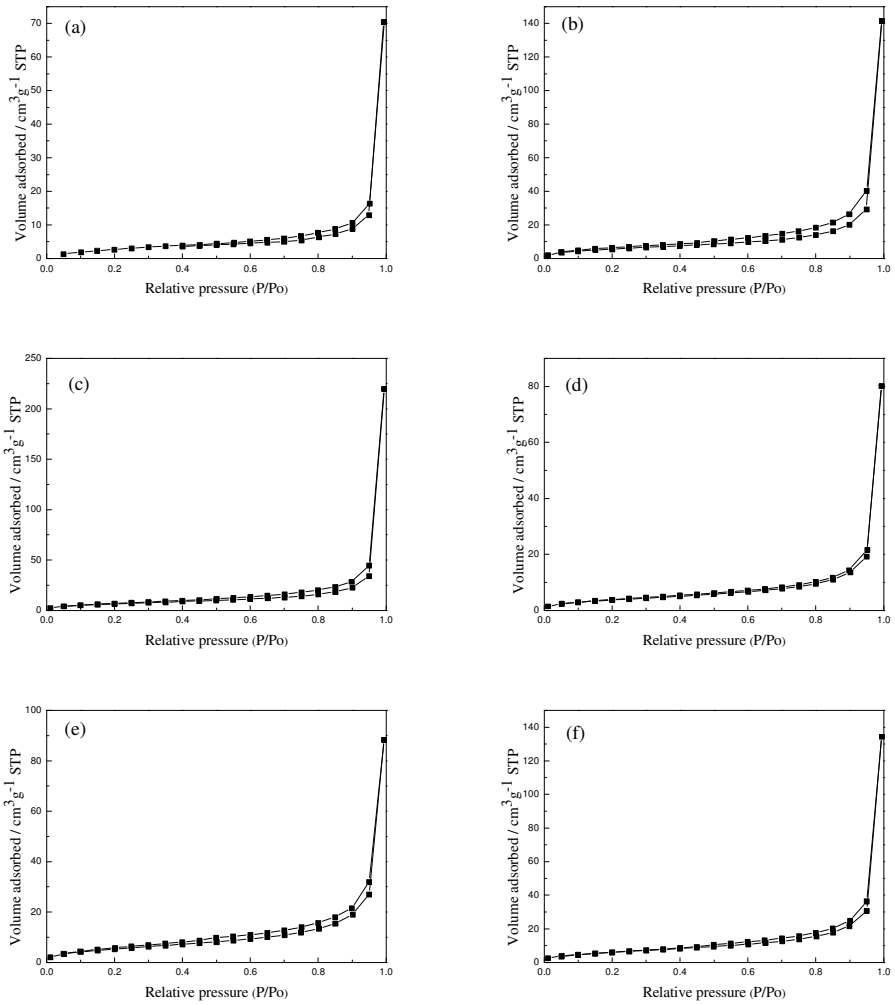

Fig. 6 Nitrogen gas adsorption and desorption isotherms (measured at 77 K) for (a) P**1**-1, (b) P**1**-2, (c) P**1**-3, (d) P**2**-1, (e) P**2**-2 and (f) P**2**-3.

The BET surface area (S_{BET}) of (a) P**1**-1, (b) P**1**-2, (c) P**1**-3, (d) P**2**-1, (e) P**2**-2 and (f) P**2**-3 were calculated by adsorption and desorption isotherms data and shown in

View Article Online
DOI: 10.1039/C6RA17790E

table **2**. The maximum BET surface area (S_{BET}) could reach 716 m^2/g. The minimum average pore size could be 21nm.

Table **2** Porosity parameters of P**1** and P**2**.

Entry	P**1**-1	P**1**-2	P**1**-3	P**2**-1	P**2**-2	P**2**-3
S_{BET} (m^2/g)	304	618	716	404	587	660
Average pore size(nm)	42	27	24	38	30	21

Compared with the adsorption ability of (a)P**1**-1, (b) P**1**-2 and (c) P**1**-3, the maximum adsorbed volume increased. P**2**-1, P**2**-2 and P**2**-3 have the same trends. It means that the maximum adsorbed volume could be tuned by adjusting the preparation conditions of the POPs. With the increase of temperature and reaction time, the high specific surfaces areas of POPs could be obtained.

3.4 Detectingmetal ions by compound 1 and compound 2

To investigate the detecting ability of the compound **1** and compound **2**, a series of experiments were conducted. Compound **1** and compound **2** turned from colorless to colored when contact with Fe(Ⅲ), Fe(Ⅱ)and Pd(Ⅱ) ions. Other heavy metal ions (Cr(Ⅲ), Mn(Ⅱ), Co(Ⅱ), Cd(Ⅱ), Zn(Ⅱ), Ag(Ⅰ), Pb(Ⅱ), Ca(Ⅱ), Ni(Ⅱ), Cu(Ⅱ), Na(Ⅰ), K(Ⅰ), Hg(Ⅱ), and Mg(Ⅱ) showed no color change. It indicated that compound **1** and compound **2**could detect Fe(Ⅲ), Fe(Ⅱ)and Pd(Ⅱ) ions. And the fluorescence became weaker when being contacted with Fe(Ⅲ), Fe(Ⅱ)and Pd(Ⅱ) ions.

View Article Online
DOI: 10.1039/C6RA17790E

Fig. S4 shows the UV–Vis spectra. The absorbance peaks of compound **1** ([Compound **1**]=5 μM) with Fe(Ⅲ), Fe(Ⅱ)and Pd(Ⅱ)ions shifted (**Fig. S4** a). It could be seen clearly the peak of about 317nm disappeared when compound **1**contacted with Fe(Ⅲ), Fe(Ⅱ)and Pd(Ⅱ)ions, the peaks of 331nm 333nm and 335nm appeared. Similarly, compound **2**([compound **2**]=5 μM) shows the same change as compound **1**(in **Fig. S4**b).

The fluorescence properties of compound **1** and compound **2**with different heavy metal ions were shown in **Fig. S5**.Taking compound **1** (**Fig. S5** (a)) as an example, the fluorescence intensity decreased when compound **1** contacted with Fe(Ⅲ), Fe(Ⅱ) and Pd(Ⅱ) ions respectively. The fluorescence changes of compound **2** were similar to compound **1** in **Fig. S5**(b). The results further demonstrated that compound **1** and compound **2** could selectively recognize Fe(Ⅲ), Fe(Ⅱ)and Pd(Ⅱ) ions by fluorescence measurement. Meanwhile, the fluorescence intensity of compound **2** gradually decreased with increasing Fe(Ⅱ) concentrations at about 426 nm (**Fig. S5** (c)). Also, from Figure S4(d), it could be seen that the fluorescence intensity of compound **2** decreased with increasing Pd(Ⅱ). And when the concentration of Pd(Ⅱ) ions lowered to 5 μM, change of color and fluorescence of compound **1** and compound **2** still could be seen.

3.5 Detecting Pd(Ⅱ) ion by P1 and P2

First, the influences of pH value to the polymer were tested using Britton-Robinson buffer solutions. And it can be seen that no notable changes in UV-Vis spectra and fluorescence spectra in the pH value range of 2 to11. Then all the experiments were

View Article Online
DOI: 10.1039/C6RA17790E

measured in the pH of 6.8 Briton-Robinson buffer solution. The sensing ability of the fluorescent P**1** and P**2** were investigated. 5 equivalent metal ion solution ((Cr(Ⅲ), Mn(Ⅱ), Co(Ⅱ), Cd(Ⅱ), Zn(Ⅱ), Ag(Ⅰ), Pb(Ⅱ), Ca(Ⅱ), Ni(Ⅱ), Cu(Ⅱ), Na(Ⅰ), K(Ⅰ), Hg(Ⅱ), Mg(Ⅱ), Fe(Ⅲ), Fe(Ⅱ) and Pd(Ⅱ)) were added to P**1** and P**2**([Polymer]=2.5μMin repeat units) suspensions at room temperature. Taking P**1** (**Fig. S6**) as an example, the color of P**1** suspension changed dramatically from yellow to orange upon addition of Pd(Ⅱ) ions, and the color of adding other ions didn't change under UV light and natural light. In **Fig. S6**, the color changed via interaction between Pd(Ⅱ) ions and P**1** rather than intrinsic color of Pd(Ⅱ) solution. Similarly, the P**2** suspension had the same change. It indicated that P**1** and P**2** could be employed to detect Pd(Ⅱ) ions as polymeric chemosensors. The mixed suspension containing metal ions and Polymer (P**1** and P**2**) were measured by the UV–Vis and fluorescence. **Fig. S7** shows the UV–Vis spectra. The absorbance peaks of P**1** with Pd(Ⅱ) ions shifted (**Fig. S7**a). It could be seen clearly the peak of about 423nm disappeared when P**1** combined with Pd(Ⅱ)ions, the peak of about 453nm appeared. Similarly, P**2** shows the same change as P**1**(**Fig. S7**b).

The fluorescence spectra (λex = 390 nm, Slit 10/20 nm) of P**1**([P**1**]=2.5μM in repeating units) were measured. As is shown in the **Fig. 7 (a)**, it can be seen fluorescence intensity decreased notably upon the addition of Pd(Ⅱ), but other metal ions did not cause any noteworthy change comparing with P**1**. P**2** shows the same change as P**1** in the **Fig. 7 (b).**As shown in **Fig. 7 (c)**, fluorescence intensity of P**1** decreased with the increasing concentration of Pd(Ⅱ) ions. Moreover, when the

View Article Online
DOI: 10.1039/C6RA17790E

concentration of Pd(Ⅱ) ions lowered to 2.5 μM, color change and fluorescence of P**1** still could be seen. As shown in **Fig. 7 (d)**, fluorescence intensity of P**2** decreased with the increasing concentration of Pd(Ⅱ) ions. And when the concentration of Pd(Ⅱ) ions lowered to 2.5 μM, color change and fluorescence of P**2** still could be seen as well.

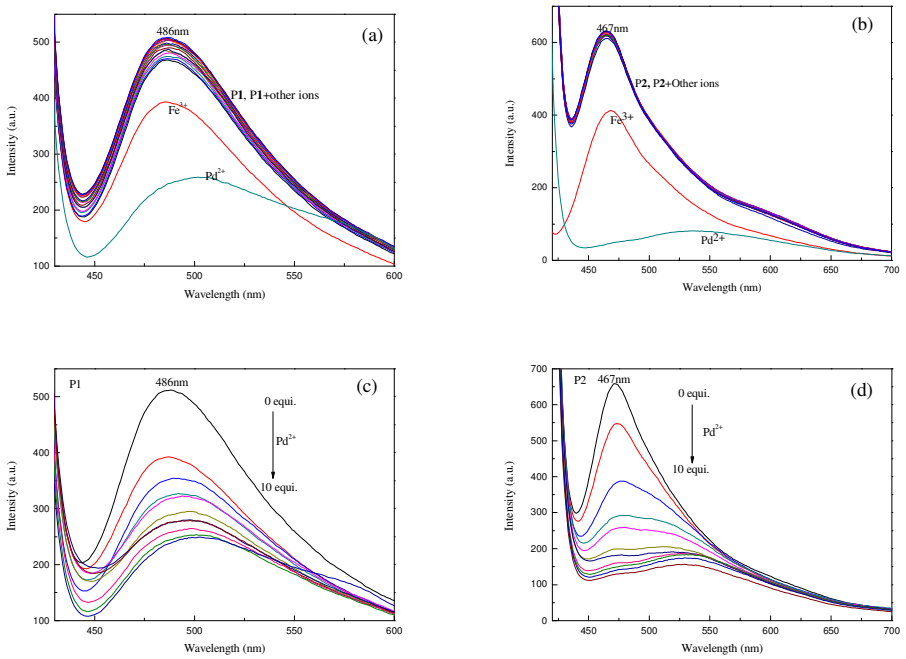

Fig. 7 Fluorescence spectra (λex = 390 nm, Slit 10/20 nm) of (a) P**1** (2.5μMin repeating units) and (b) P2 (2.5μm in repeating units) with different heavy metals ions ((Cr(Ⅲ), Mn(Ⅱ), Co(Ⅱ), Cd(Ⅱ), Zn(Ⅱ), Ag(Ⅰ), Pb(Ⅱ), Ca(Ⅱ), Ni(Ⅱ), Cu(Ⅱ), Na(Ⅰ), K(Ⅰ), Hg(Ⅱ), Mg(Ⅱ), Fe(Ⅲ), Fe(Ⅱ) and Pd(Ⅱ)) in DMF/water, (c) P 1 with different concentration of Pd(Ⅱ) ions and (d) P**2** with different concentration of Pd(Ⅱ) ions.

To make clear whether other metal ions have interference to the detection of Pd(Ⅱ) ions, equivalent other every mental ions with Pd(Ⅱ) ions were simultaneously added

View Article Online
DOI: 10.1039/C6RA17790E

to the P**1** and P**2**suspension. The results indicated that they have no interference to the recognition of Pd(Ⅱ)(**Fig. 8**).

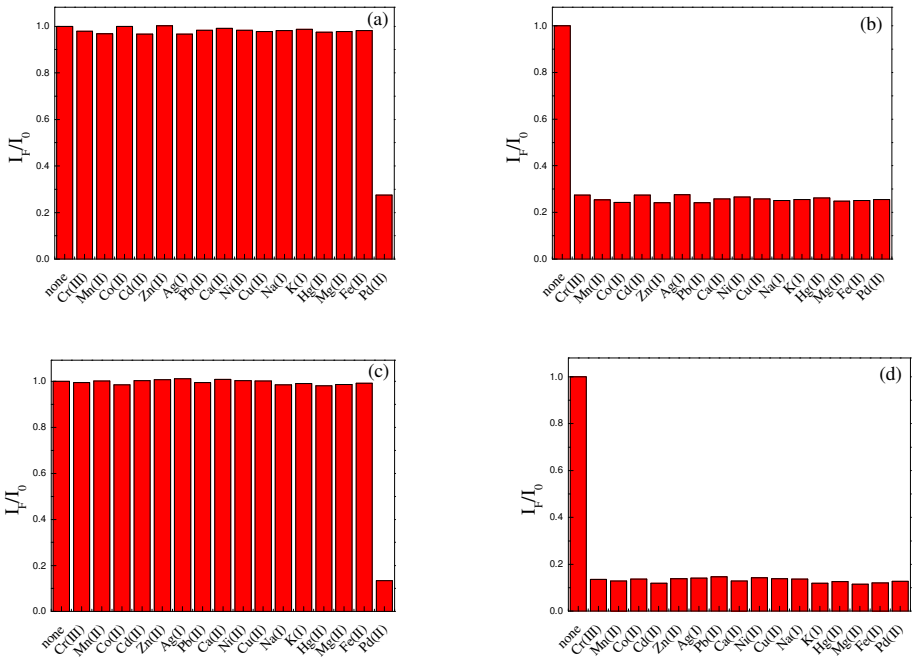

Fig. 8 Fluorescent response of P**1** (2.5μM) and P**2** (2.5μM) with metal ions (5μM). (a) P**1** with single metal ions, (b) P**1** with other metal ions and Pd(Ⅱ), (c)P**2** with single metal ions, (d) P**2** with other metal ions and Pd(Ⅱ).

3.6 Adsorption of RhB and MB

Adsorption of Methylene blue and Rhodamine B by P**1** and P**2** for were measured at room temperature. The adsorption efficiency of P**1** and P**2** serieswere measured as follows. Added a series of P**1** (5mg) to 5mL RB solution (0.01g/L), adsorption equilibrium could be reached within 5min. The adsorption percentages of P**1** series after 5min were as follows: 40.6% for P**1**-1, 86.0% for P**1**-2, 87.9% for P**1**-3and 98.2% for P**1**-4 respectively in the **Fig. 9** (a). Similarly, the adsorption percentages of P**2** series after 5min were as follows: 39.3% for P**2**-1, 82.4% for P**2**-2, 89.0% for P**2**-3

View Article Online
DOI: 10.1039/C6RA17790E

and 98.6% for P**2**-4 respectively and shown in **Fig. 9** (c). Using the same method, double weight of P**1** and P**2** experiments were conducted. As shown in **Fig. 9** (b) and (d), the adsorption percentages of P**1** and P**2** for RhB solution after 5min were as follows: 56.5% and 61.1% for P**1**-1 and P**2**-1, 91.8% and 89.0% for P**1**-2 and P**2**-2, 92.1% and 90.1% for P**1**-3 and P**2**-3, 98.9% and 98.6% for P**1**-4 and P**2**-4 respectively. And the adsorption efficiency of P**1** and P**2** for RhB was very close. The adsorption efficiency can reach to 98.9% within 5min.

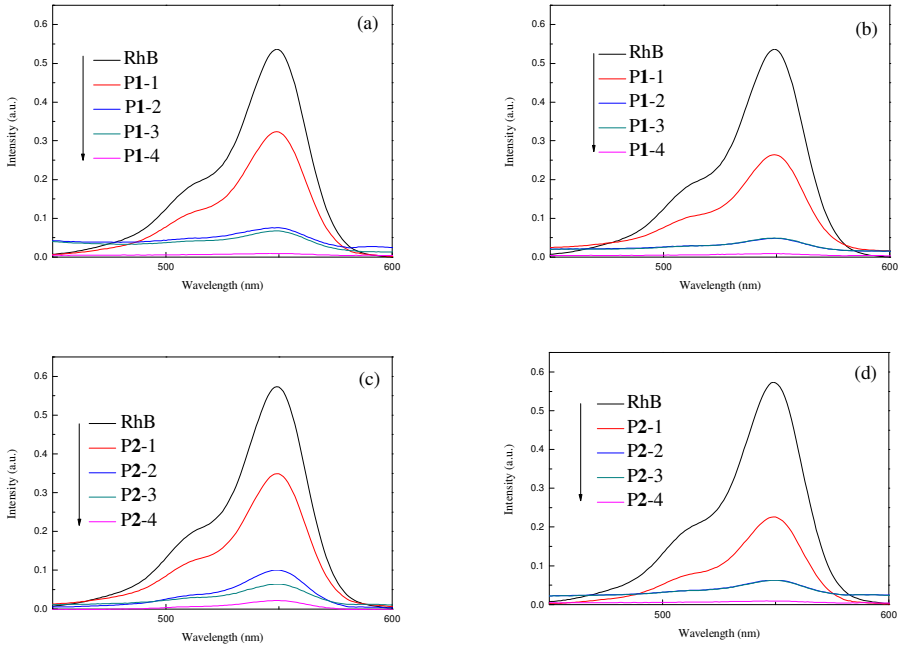

Fig. 9 Adsorption of P**1** and P**2** for Rhodamine B: (a) 5mg P**1**, (b) 10mg P**1**, (c) 5mg P**2** and (d) 10mg P**2**.

Different POPs were used to study the dye adsorption abilities. Namely, P**1**-1 to P**1**-4, P**2**-1 to P**2**-4 were used and the results were shown in **Fig. 9**. Both the P**1** and P**2** series shown the same trends. The POPs obtained at higher temperature and longer reaction time, the higher dye adsorption abilities obtained. In other words, P**1**-4 and

View Article Online
DOI: 10.1039/C6RA17790E

P**2**-4 are the best ones. In this experiment, change the weight of POPs from 5mg to 10mg. the results showed that there were no notable efficiency increase between 5mg to 10mg POPs. Which means that 5mg POP is enough to adsorb the RhB. As for the adsorption of MB, the results are shown in **Fig 10**.It can be seen that under the same conditions, RhB is much easier be adsorbed than MB. The maximum adsorption efficiency for MB only 58.78%. It indicated the adsorption capacity of POPs were different for different dyes.

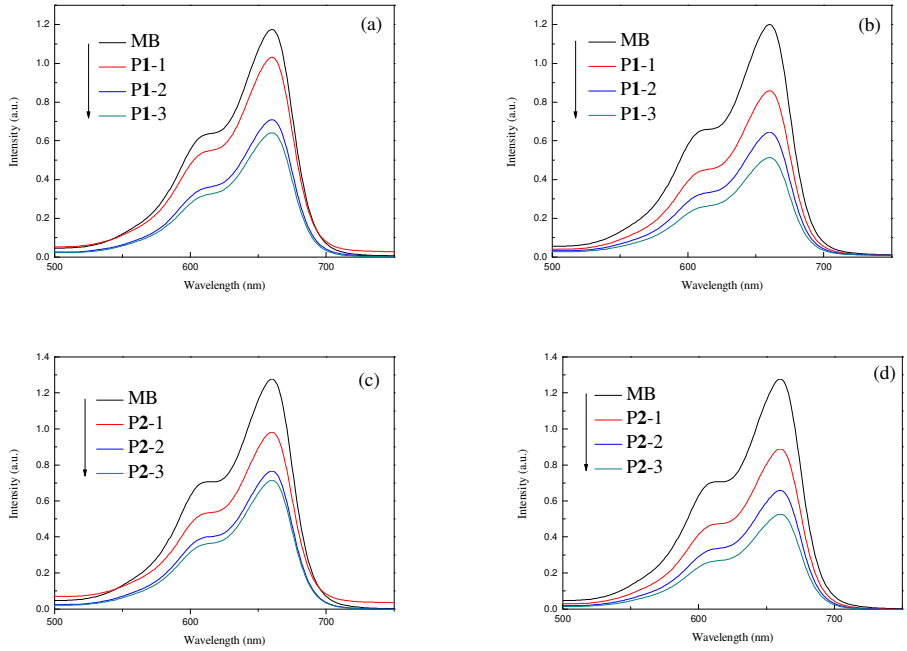

Fig. 10 Adsorption of P**1** and P**2** for Methylene blue: (a) 5mg P**1**, (b) 10mg P**1**, (c) 5mg P**2** and (d) 10mg P**2**.

As shown in the **Fig. 11** (a) and (b), the colors of RhB and MB faded with the addition of P**1**. As shown in Fig.11, the color of P**1** and P**2** powders changed from yellow to orange and green, which indicated the adsorption of the organic dyes.

View Article Online
DOI: 10.1039/C6RA17790E

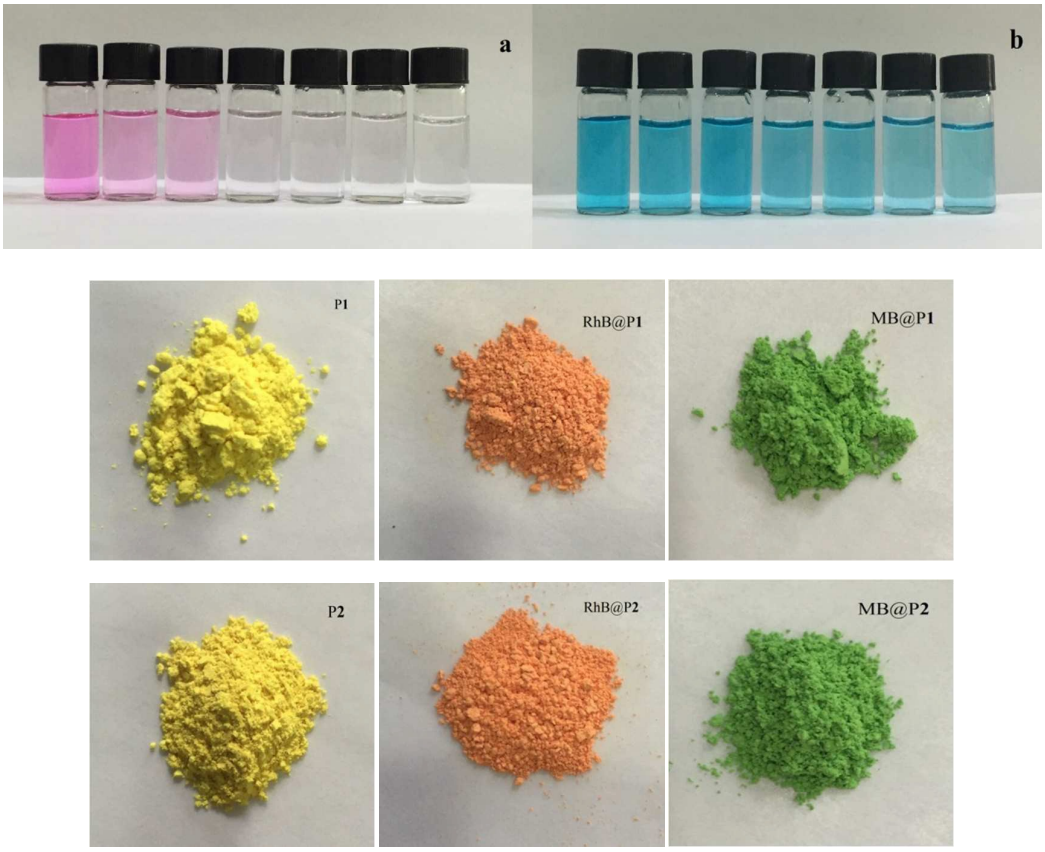

Fig. 11the color change (a) Rhodamine B and (b) Methylene bluebefore and afteradsorbed by P**1**.the color change of P**1** and P**2** before and after adsorb Rhodamine B and Methylene blue.

3.7 Adsorption of Pd(Ⅱ)

The adsorptions of Pd(Ⅱ)were measured at room temperature. First, Pd(Ⅱ) solution (10.64 mg/L) were prepared. 5mg and 10mg of P**1** (P**1**-1 to P**1**-4) and P2 (P**2**-1 to P**2**-4) were added to 10mL Pd(Ⅱ) solution and stirred for 5min. The concentrations of Pd(Ⅱ) before and after the addition of P**1** and P**2** were measured by AAS. The adsorption performance of Pd(Ⅱ) ions on P**1** and P**2** were calculated by the following formula,

$$E_f = \frac{C_0 - C_e}{C_0} \times 100\% \qquad (1)$$

View Article Online
DOI: 10.1039/C6RA17790E

$$Q = \frac{(C_0 - C_e) \times V}{m} \quad (2)$$

where E_f, Q, C_0, C_e, V and m represent the adsorption efficiency (%), the adsorption capacity (mg/g), the original concentration of Pd(Ⅱ) ions, the equilibrium concentration of Pd(Ⅱ) ions, and the total volume and the quality respectively. The adsorption performance of Pd(Ⅱ) ions on P**1** and P**2** was calculated by equations (1) and (2). The results were presented in the table 3.

Table 3 Adsorption efficiency (E_f) and adsorption capacity (Q) of different condition of P**1** with Pd(Ⅱ) ions.

Entry	POP (mg)	C_0(mg/L)	C_e (mg/L)	E_f(%)	Q (mg/g)
P**1**-1	5	10.64	6.5645	38.3	8.2
P**1**-2	5	10.64	3.6822	65.4	14.0
P**1**-3	5	10.64	3.149	70.4	15.0
P**1**-4	5	10.64	1.0532	90.1	19.2
P**1**-1	10	10.64	3.661	65.6	7.0
P**1**-2	10	10.64	2.2888	78.5	8.4
P**1**-3	10	10.64	1.6919	84.1	8.9
P**1**-4	10	10.64	0.1082	99.0	10.5
P**2**-1	5	10.64	6.2056	41.7	8.9
P**2**-2	5	10.64	2.214	79.2	16.9
P**2**-3	5	10.64	1.9295	81.9	17.4
P**2**-4	5	10.64	0.3194	97.0	20.6

View Article Online
DOI: 10.1039/C6RA17790E

P**2**-1	10	10.64	3.376	68.3	7.3
P**2**-2	10	10.64	0.7364	93.1	9.9
P**2**-3	10	10.64	0.3299	96.7	10.3
P**2**-4	10	10.64	0.2349	97.8	10.4

It could be concluded that P1-4 and P2-4 are the best ones concerning the adsorption efficiency and capacity.

4. Conclusions

In conclusion, two kinds of porous organic polymers were synthesized. They are layer-nanosheet structured, fluorescent and crystalline. The pore diameters and specific surface areas of the POPs could be tuned by changing the reaction time and temperature. The POP nanosheet showed relatively high thermal stability. They could be used to adsorb organic dyes and Pd(Ⅱ) ions.Under longer reaction time and higher temperatures, POPs with larger specific surface areas and smaller pore size could be obtained. And these POPs have the best adsorption efficiency and capacity. They might find real applications in the treatment of dye and metal ion pollutions in the future.

Acknowledgements: The authors thank financial support of National Natural Science Foundation of China (NSFC No. 41573106).

View Article Online
DOI: 10.1039/C6RA17790E

References

[1] C. Özdemir, Ş. Saçmacr, Ş. Kartal, M. Saçmacr,*J. Ind. Eng. Chem.* **2014**, *20*, 4059.

[2]. M. R. Awual, T. Yaita, S. A. El-Safty, H. Shiwaku, Y. Okamoto, S. Suzuki,*Chem. Eng. J.* **2013,** *222*, 172.

[3] W. X. Ren, T. Pradhan, Z. G. Yang, Q. Y. Cao, J. S. Kim,*Sensor Actuat B: Chem.***2012**,*171*, 1277.

[4] K. V. Meel, A. Smekens, M. Behets, P. Kazandjian, R. V. Grieken, *Anal. Chem.* **2007**, *79*, 6383.

[5]M. Ezoddin, K. Abdi, N. Lamei, *Talanta***2016**, *153*, 247.

[6]Z. Y. Xu, X. L. Wang, J. W. Yan, J. Li, S. Guan, L. Zhang, *RSC Adv.* **2016**, *6*, 43539.

[7] J. H. Ran, H. Y. Wang, X. J Cheng,*J Mater Sci*.**2016**, *51*, 8502.

[8] B. Liu, Y. Y. Bao, H. Wang, F. F. Du, J. Tian, Q. B. Li, T. S. Wang, R. K. Bai,*J. Mater. Chem.* **2012**, *22*, 3555.

[9] B. Liu, H. G. Dai, Y. Y. Bao, F. F Du, J. Tian, R. K. Bai, *Polym. Chem.***2011**,*2,* 1699.

[10] Y. M. Luo, Y. R. Jia, D. X. Zhang, X. J. Cheng, *Photochem. photobiol.***2016**,*92*, 515.

[11] C. K. Wang, F. F. Xing, Y. L. Bai, Y. M. Zhao, M. X. Li, S. R. Zhu, *Cryst. Growth Des.***2016**, *16*, 2277.

View Article Online
DOI: 10.1039/C6RA17790E

[12] X. Zhu, C. C. Tian, S. M. Mahurin, S. H. Chai, C. M. Wang, S. Brown, G. M. Veith, H. M. Luo, H. L. Liu, S. Dai, *J. Am. Chem. Soc.* **2012**, *134*, 10478.

[13] S. W. Yuan, B. Dorney, D. White, S. Kirklin, P. Zapol, L. P. Yu, D. J. Liu, *Chem. Commun.***2010**, *46*, 4547.

[14] P. Kuhn, K. Krüger, A. Thomas, M. Antonietti, *Chem. Commun.* **2008**, *44*, 5815.

[15] N. B. McKeown, P. M. Budd, *Chem. Soc. Rev.* **2006**, *35*, 675.

[16] G. Y. Li, B. Zhang, Z. G. Wang, *Macromolecules* **2016**, *49*, 2575.

[17] V. M. Suresh, S. Bonakala, H. S. Atreya, S. Balasubramanian, T. K. Maji, *ACS Appl. Mater. Interfaces.***2014**, *6,* 4630.

[18] Y. Z. Liao, J. Weber, C. F. J.Faul, *Macromolecules***2015**, *48*, 2064.

[19] M. Liras, M. Iglesias, Sánchez, F, *Macromolecules***2016,***49*, 1666.

[20] A. M. Shultz, O. K. Farha, J. T. Hupp, S. T. Nguyen, *Chem. Sci.***2011**, *2*, 686.

[21] J. X. Jiang, C. Wang, A. Laybourn, T. Hasell, R. Clowes, Y. Z. Khimyak, J. L. Xiao, S. J. Higgins, D. J. Adams, A. I. Cooper, *Angew. Chem. Int. Ed.***2011**, *50*, 1072.

[22] S. Hug, M. E. Tauchert, S. Li, U. E. Pachmayr, B. V. Lotsch, *J. Mater. Chem.***2012**, *22*, 13956.

[23] J. S. Yang, T. M. Swager, *J. Am. Chem. Soc.***1998**, *120*, 11864.

[24] Y. W. Zhang, S. A, Y. C. Zou, X. L. Luo, Z. P. Li, H. Xia, X. M. Liu, Y. Mu, *J. Mater. Chem. A***2014**, *2*, 13422.

[25] T. M. Geng, H. Zhu, W. Song, F. Zhu, Y. Wang, *J. Mater. Sci.* **2016**, *51*, 4104.

[26] L. Chen, Y. Honsho, S. Seki, D. L. Jiang, *J. Am. Chem. Soc.* **2010***, 132,* 6742.

View Article Online
DOI: 10.1039/C6RA17790E

[27] Y. H. Xu, L. Chen, Z. Q. Guo, A. Nagai, D. L. Jiang, *J. Am. Chem. Soc.***2011**, *133,* 17622.

[28] J. X. Jiang, A. Trewin, D. J. Adams, *Chem. Sci.***2011**, *2*, 1777.

[29] X. M. Liu, Y. H. Xu, D. L. Jiang,*J. Am. Chem. Soc.***2012**, *134,* 8738.

[30] J. Wei, X. M. Zhang, Y. P. Zhao, R.X.Li, *Macromol. Chem. Phys.***2013**, *214,* 2232.

[31] Q. Chen, D. P. Liu, M. Luo, L. J. Feng, Y. C. Zhao, B. H. Han, *Small*. **2014**, *2*, 308.

[32] A. Patra, J. M. Koenen, U. Scherf, *Chem. Commun.***2011**, *47*, 9612.

[33] H. Lim, J. Y. Chang, *Macromolecules***2010**, *43*, 6943.

[34] W. Huang, C. T. Gu, T. Wang, C. Y. Gu, S. L. Qiao, R.Q.Yang, *RSC Adv*. **2014**, *4*, 62525.

[35] J. R. Song, Z. T. Huang, Q. Y. Zheng, *Chin. J. Chem.***2013**, *31*, 577.

[36] L. H. Xie, M. P. Suh, *Chem. Eur. J.***2013**, *19*, 11590.

[37] G.J. Chang, Z.F. Shang, T. Yu, L. Yang, *J. Mater. Chem. A.***2016**, *4*, 2517.

[38] H. Li, X. S. Ding, Y. C. Zhao, B. H. Han, *Polymer.***2016**,*89*, 112.

[39] O. Prakash, H. Joshi, K. N. Sharma, A. K. Sharma, A. K. Singh, *Eur. J. Inorg. Chem.* **2015**, *3*,520.

[40] H. Zhang, W. Q. Ding, K. He, M. Li, *Nanoscale Res. Lett.***2010**,*5*, 1264.

[41] T. Kasuga, M. Hiramatsu, A. Hoson, T. Sekino, K. Niihara, *Langmuir.* **1998**, *14*, 3160.

View Article Online
DOI: 10.1039/C6RA17790E

Graphic Abstract

Text for Table of Contents

Two kinds of layer-nanosheet POPs were synthesized. They exhibit unique porous structures and considerable specific surface areas. The specific surface area and pore diameters could be adjusted via changing the reaction time and temperature. The POPs exhibit high adsorption capacity for RhB, MB and Pd(Ⅱ) ions.

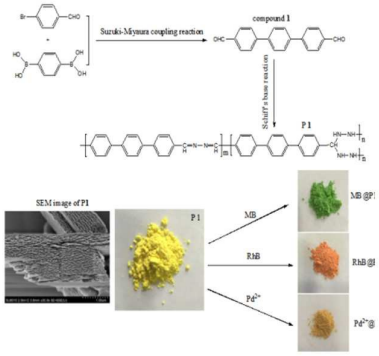

*Yanmei Luo, Junhui Ran, Rong Chen, and Xinjian Cheng**

Facile Synthesis of Porous Organic Polymers for the Absorption of Pd(Ⅱ) Ions and Organic Dyes